$$\frac{\nu_b \mu_{jb}^2}{\nu_b^2 - \nu_a^2}$$

for the substituent and the reference substituent of Table III. For example, a $C_3'$–S (*cis*) bond is predicted to contribute substantially in a negative sense to the rotation (about eight times more than the $-0.55 \times 10^{-40}$ cgs contribution of the $C_3'$–O (*cis*) bond). Hence 3′-thioxylofuranosyluracil is predicted to exhibit a much smaller positive $B_{2u}$ Cotton effect than 1-(β-D-xylofuranosyl)uracil. On the other hand 3′-mercapto-3′-deoxyuridine should give a $B_{2u}$ Cotton effect only slightly larger than the corresponding Cotton effect of uridine since eight times the contribution of a $C_3'$–O *trans* bond, *i.e.*, $8 \times 0.04 \times 10^{-40}$, still does not add an appreciable amount of the total $B_{2u}$ rotation. Similarly 2′-thioarabinofuranosyluracil is expected to have a very large positive $B_{2u}$ Cotton effect where as the 2′-*trans* isomer may well have a negative $B_{2u}$ Cotton effect. Thus the configuration at C-2′ and C-3′ for a sulfur substituent should be rather easily determined by CD measurements.

In summary, the coupled oscillator term in the general expression for the rotational strength describes on a relative basis most of the changes in the $B_{2u}$ Cotton effect due to changes in the nature and geometry of the vicinal oscillators. The agreement is indeed very good for *R*-configuration nucleosides for which X-ray data are available, but several exceptions are noted for *S*-configuration nucleosides, which may serve to indicate that the sugar-base conformation or the specific sugar conformation is influenced by the C-1′ configuration. Although there are a few instances where an individual vicinal bond has shown a divergent contribution from experimental data, this has never been sufficiently pronounced to lead to a wrong assignment of the absolute configuration. In the three cases where the theoretical vicinal contribution of one bond differed in sign from the experimental value, the exact configuration is problematical due to lack of X-ray data on these structures.

Inclusion of contributions from the other terms to the rotational strength may improve the calculations but, on a practical basis, the results of this paper show that many problems regarding nucleoside stereochemistry may be solved by appealing solely to the bond–bond coupled oscillator theory. The success of the theoretical calculations reported here depend on giving up the Kirkwood–Tinoco method where the base chromophore is considered as a single oscillator. In the bond–bond coupled oscillator theory each transition of the base chromophore is resolved into contributions from the individual bonds. Thus the geometry of the chromophore and its disposition relative to the vicinal oscillators are introduced into the calculations. This procedure is essential for the success of the theory. Several previously published methods were tried without notable success, including the method in which the transition of the base chromophore is resolved into transition monopoles to calculate the potential.[10]

**Acknowledgment.** The authors wish to thank Khosrow Semnani and Clark Miles for excellent technical assistance. This work was supported by the National Institutes of Health Grant No. GM 12862-05 and the Petroleum Research Fund Grant No. PRF 253-C.

# Spin Label Studies of Oriented Smectic Liquid Crystals[1] (A Model System for Bilayer Membranes)

**Joachim Seelig**[2]

*Contribution from the Stauffer Laboratory for Physical Chemistry, Stanford, California 94305.* *Received December 11, 1969*

**Abstract:** Smectic liquid crystals with bilayer structure can be homogeneously oriented between two parallel glass surfaces. Spin labels dissolved in this system are found to undergo a rapid, anisotropic motion. The esr spectrum depends on the orientation of the sample with respect to the applied magnetic field. The formulas necessary for a quantitative evaluation of the spin label spectra are derived. Amphiphilic spin labels and steroid spin labels are used to investigate the different regions of the bilayer. The amphiphilic spin labels indicate an exponential decrease in the degree of order, when the distance between the carboxyl group and the spin label group is increased. In spite of this flexibility, the amphiphilic materials of the bilayer are found to be in an almost extended configuration. The behavior of the spin labels in phospholipid dispersions is very similar to that in the liquid crystalline model system.

In recent years the spin labeling technique has been introduced as a method in the elucidation of the structure of biological membranes.[3] Progress in this field has been made by the synthesis of spin labels which show a rapid and highly anisotropic motion in biological membrane systems.[4,5] It has been suggested that the anisotropic motion of these labels can be attributed to their incorporation into a bilayer structure.

Here we wish to report spin label experiments in

(1) Work supported by the National Science Foundation under Grant No. GP 9315.

(2) Fellow of the Deutsche Forschungsgemeinschaft, 1968–1969. After January 1, 1970, address correspondence to the author at Institut für Physikalische Chemie, Universität Basel, 4056 Basel, Switzerland.

(3) H. M. McConnell and B. G. McFarland, *Quart. Rev. Biophys.*, in press.

(4) W. L. Hubbell and H. M. McConnell, *Proc. Nat. Acad. Sci. U. S.*, **63**, 16 (1969).

(5) W. L. Hubbell and H. M. McConnell, *ibid.*, in press.

which a model system having a known bilayer structure was used. These studies have provided more detailed information about the nature of the anisotropic motion of spin labels and, in addition, information about the physical state of the bilayer. This more sophisticated picture is possible because of two facts. (1) We have introduced a model system which, compared with biological membranes, has the following advantages: (a) the chemical composition of this system is simple and well defined; (b) the geometric structure is known by X-ray analysis; (c) as will be described in detail in the following sections, it is possible to obtain a homogeneous orientation of the bilayer system which, in turn, leads to a homogeneous ordering of incorporated spin labels. The esr spectrum then consists of three relatively sharp lines and the **g** and **T** tensors become dependent on the angle between the magnetic field and the unique axis of orientation. This angle can be varied arbitrarily. Because of the homogeneous orientation of the spin labels it is possible to detect even very small degrees of anisotropic rotation. (2) We have synthesized a series of spin-labeled fatty acids, which are very similar to the amphiphilic materials of our model system, and where the distance between the carboxyl group and the position of the spin label group has been systematically varied.

The concluding step in this report will be a comparison between the model system and phospholipid dispersions with bilayer structure.

## I. The Model System

A study by Mandell, *et al.*,[6] has shown that mixtures of sodium decanoate, *n*-decyl alcohol, and water can form a number of structurally different liquid crystalline phases at room temperature. In their phase diagram the region designated D is of special interest to us, because it has a typical bilayer structure: the microcrystalline regions consist of layers of amphiphilic materials separated by layers of water. The polar head groups of the amphiphilic substances are in contact with the water phase, while the hydrocarbon tails stick together to form a hydrophobic core. The hydrocarbon chains are all identical and completely saturated. The thickness of one bilayer—as determined by X-ray crystallography—amounts to 22–24 Å. The spacing between two adjacent double layers depends very much on the water content of the mixtures and varies from 7 to 80 Å.

We have chosen phase D as a model system for our spin label experiments. The liquid crystals can easily be prepared by cooling down an isotropic solution of appropriate composition. The system is stable at room temperature and with the exception of its geometrical structure has no unusual features. The actual chemical composition of our system was

| | |
|---|---|
| sodium decanoate | 28 wt % |
| decanol | 42.1 wt % |
| water | 29.9 wt % |

Phase D is a true smectic phase as defined by Friedel.[7] One common property of this type of liquid crystal is the high mobility of the double layers with respect to each other; *i.e.*, they slide on each other without much friction. This leads to a macroscopic ordering of the smectic phase, when it is forced between two closely spaced, parallel glass surfaces. Shearing forces and the contact with the glass surfaces arrange the microcrystalline regions in parallel layers on the supporting plates, thus repeating their molecular order on a macroscopic scale. The system now has a unique axis of orientation, which is identical with the normal of the glass plates. This axis becomes the optical axis of the liquid crystalline system. It is therefore possible to observe the ordering process by means of a polarizing microscope.

Using two cover slides, we could easily demonstrate this pseudoisotropy for phase D. We have taken advantage of this orientation phenomenon in our esr measurements. Using a rectangular quartz cell with the dimensions 4.5 × 1.0 × 0.005 cm it was possible to get an almost homogeneous orientation of the smectic phase. The next question, therefore, is how this ordering will affect the esr spectrum of a spin label incorporated into the smectic phase.

## II. The Esr Spectrum of Spin Labels in Oriented Smectic Liquid Crystals

Nematic liquid crystals are well-known solvents in nmr and esr spectroscopy.[8] In a magnetic field the rod-like molecules of the nematic phase are aligned more or less parallel to the field axis, forcing the solute molecules in the same direction. From the change in the solute spectrum valuable information can be deduced about the orientation of the solute molecules in the nematic phase and about their geometry. Studies of spin labels in nematic phases have been made by Falle, *et al.*,[9] and by Ferruti, *et al.*[10]

However, only a few examples have been reported, where smectic phases have been used as solvent systems.[11] Smectic liquid crystals are less fluid than nematic ones and, once formed, will not be oriented by a magnetic field. Nevertheless, there is still a rapid molecular motion in the smectic phase. This motion is highly anisotropic and the average motion of each molecule in an oriented sample shows rotational symmetry with respect to the optical axis.

Bearing this in mind, we may proceed to give the following description of the label spectrum in an oriented smectic phase. The essential group in our spin labels is the NO radical. We ascribe a Cartesian coordinate system $x$, $y$, $z$ to the NO group such that the $x$ axis is extended in the direction of the NO bond and the $z$ axis in the direction of the nitrogen $2p\pi$ orbital. Within this molecular frame the hyperfine splitting is described by an axial symmetric tensor **T**.[12]

$$\mathbf{T} = \begin{pmatrix} T_{xx} & 0 & 0 \\ 0 & T_{xx} & 0 \\ 0 & 0 & T_{zz} \end{pmatrix} \qquad (1)$$

A second coordinate system $\xi$, $\eta$, $\zeta$ is related to the

(6) L. Mandell, K. Fontell, and P. Ekwall, Advances in Chemistry Series, No. 63, American Chemical Society, Washington, D. C., 1967, p 89.

(7) G. Friedel, *Ann. Phys.* (Paris), **18**, 273 (1922).

(8) A. Saupe, *Angew. Chem., Int. Ed. Engl.*, **7**, 97 (1968).

(9) H. R. Falle, G. R. Luckhurst, H. Lemaire, Y. Marechal, A. Rassat, and P. Rey, *Mol. Phys.*, **11**, 49 (1966).

(10) P. Ferruti, D. Gill, M. A. Harpold, and M. P. Klein, *J. Chem. Phys.*, **50**, 4545 (1969).

(11) *E.g.*, C. S. Yannoni, *J. Amer. Chem. Soc.*, **91**, 4611 (1969).

(12) C. L. Hamilton and H. M. McConnell in "Structural Chemistry and Molecular Biology," A. Rich and N. Davidson, Ed., W. H. Freeman and Co., San Francisco, Calif., 1968.

oriented smectic phase. Here the $\zeta$ axis shall coincide with the optical axis of the liquid crystalline system. Transforming **T** into the $\xi$, $\eta$, $\zeta$ system and taking into account that molecular motion leads to an average tensor **T'**, which is invariant against rotation around the $\zeta$ axis

$$\mathbf{T}' = \begin{pmatrix} T_\perp & 0 & 0 \\ 0 & T_\perp & 0 \\ 0 & 0 & T_\parallel \end{pmatrix} \tag{2}$$

with the elements

$$T_\perp = (1/2)(1 + \langle\cos^2\theta_3\rangle)T_{xx} + (1/2)(1 - \langle\cos^2\theta_3\rangle)T_{zz} \tag{3}$$

$$T_\parallel = (1 - \langle\cos^2\theta_3\rangle)T_{xx} + \langle\cos^2\theta_3\rangle T_{zz} \tag{4}$$

$\theta_3$ is the angle between the $z$ and $\zeta$ axes; $\langle\cos^2\theta_3\rangle$ therefore determines the mean square deviation of the nitrogen $2p\pi$ orbital from the optical axis. The degree of order of the $z$ axis with respect to the $\zeta$ direction is defined by

$$S_3 = (1/2)(3\langle\cos^2\theta_3\rangle - 1) \tag{5}$$

Combining eq 3 and 4 results in a very convenient expression for the experimental determination of $S_3$.

$$S_3 = (T_\parallel - T_\perp)/(T_{zz} - T_{xx}) \tag{6}$$

The hyperfine splitting $T_\parallel$ ($T_\perp$) is the splitting observed when the optical axis is parallel (perpendicular) to the magnetic field. In the general case, where the optical axis makes an angle $\varphi$ with the magnetic field, the following equation for the hyperfine splitting is obtained.

$$T_{obsd} = (T_\parallel^2 \cos^2\varphi + T_\perp^2 \sin^2\varphi)^{1/2} \tag{7}$$

From the invariance of the trace of a tensor against coordinate transformations it follows that

$$2T_\perp + T_\parallel = 2T_{xx} + T_{zz} = 3a \tag{8}$$

where $a$ is the isotropic splitting constant. $T_\perp$ and $T_\parallel$ are experimental values; therefore $a$ can be determined immediately from eq 8. Changes in the polarity of the environment of the NO radical should affect $T_{xx}$ and $T_{zz}$ in the same way. In a first approximation

$$T_{xx}/T_{zz} = \text{constant} = 0.188 \tag{9}$$

as determined from single-crystal studies.[12] Using this assumption it is possible to derive quite accurate values for the elements in **T**, which can then be used to calculate $S_3$ (*cf.* section IV, Table II).

An analogous derivation can be given for the **g** tensor. In the $x$, $y$, $z$ system the **g** tensor has diagonal symmetry.[12]

$$\mathbf{g} = \begin{pmatrix} g_{xx} & 0 & 0 \\ 0 & g_{yy} & 0 \\ 0 & 0 & g_{zz} \end{pmatrix} \tag{10}$$

The average tensor **g'** in the liquid crystalline phase must have axial symmetry with respect to $\zeta$

$$\mathbf{g}' = \begin{pmatrix} g_\perp & 0 & 0 \\ 0 & g_\perp & 0 \\ 0 & 0 & g_\parallel \end{pmatrix} \tag{11}$$

The elements $g_\perp$ and $g_\parallel$ can be expressed as

$$g_\perp = (1/2)(1 - \langle\cos^2\theta_1\rangle)(g_{xx} - g_{yy}) + (1/2)(1 - \langle\cos^2\theta_3\rangle)(g_{zz} - g_{yy}) + g_{yy} \tag{12}$$

$$g_\parallel = \langle\cos^2\theta_1\rangle(g_{xx} - g_{yy}) + \langle\cos^2\theta_3\rangle(g_{zz} - g_{yy}) + g_{yy} \tag{13}$$

$\theta_1$ is the angle between the $x$ and the $\zeta$ axes. $S_1$, the degree of order of the $x$ axis, is then given by the expression

$$S_1 = (1/2)(3\langle\cos^2\theta_1\rangle - 1) = \{3g_\parallel - (g_{xx} + g_{yy} + g_{zz}) - 2S_3(g_{zz} - g_{yy})\}/2(g_{xx} - g_{yy}) \tag{14}$$

From the invariance of the tensor trace it follows that

$$2g_\perp + g_\parallel = g_{xx} + g_{yy} + g_{zz} \tag{15}$$

If approximate values for the differences $(g_{zz} - g_{yy})$ and $(g_{xx} - g_{yy})$ are taken from single-crystal studies,[12] measurement of **g'** and **T'** together allows a complete description of the orientation of the NO group in the smectic phase. $S_2$, which determines the angle between $y$ and $\zeta$, is fixed by the relation

$$S_1 + S_2 + S_3 = 0 \tag{16}$$

## III. The Spin Labels

Most of our experiments have been performed with spin labels of the following structure.

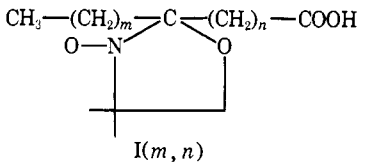


I($m$, $n$)

Since these labels are derivatives of fatty acids, their physical and chemical behavior resembles very much that of the amphiphilic components of our model system. The distance of the label group from the carboxyl end was varied in order to examine the different regions of the bilayer phase.

The oxazolidine ring attaches the NO group rigidly to the hydrocarbon chain, and the nitrogen $2p\pi$ orbital will be oriented parallel to the long molecular axis, if the chain is frozen in a planar all-*trans* configuration. As the molecular motion increases, the flexibility of the carbon skeleton will gradually diminish this orientation effect.

The following spin labels of type I($m$,$n$) have been used

| | |
|---|---|
| I(13, 2)<br>I(12, 3)<br>I(9, 6)<br>I(5, 10) | stearic acid |
| I(17, 3) | tricosanoic acid |
| I(0, 2) | levulinic acid |

Additional experiments have been made with the steroid labels IIa and IIb.[4]

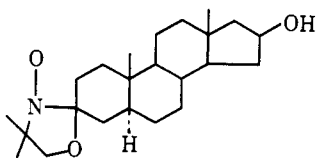


IIa

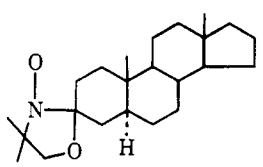


IIb

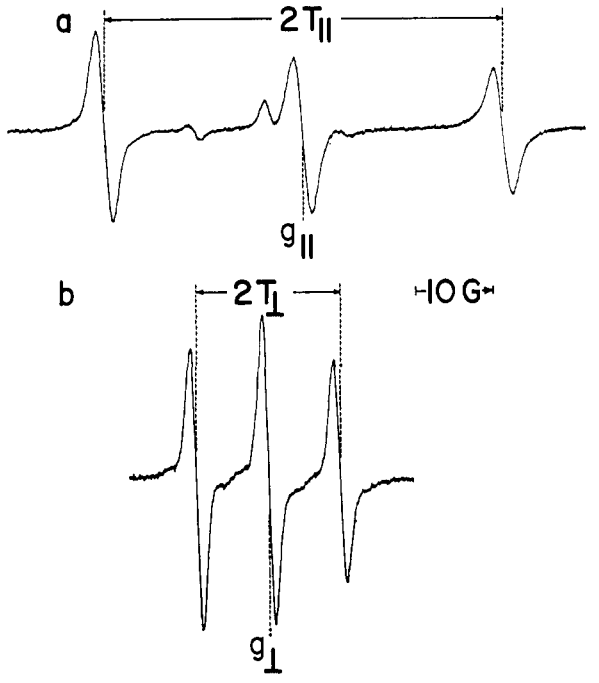


Figure 1. Spin label I(13, 2) in an oriented sample of smectic liquid crystals: (a) applied magnetic field parallel to the optical axis, (b) applied magnetic field perpendicular to the optical axis.

These labels are different from type I not only by their rigid structure but in that the nitrogen $2p\pi$ orbital is perpendicular to the long molecular axis.[4] In label IIa the more hydrophilic end is determined by the OH group, whereas in IIb the oxazolidine ring is the only polar region.

**Synthesis of Label I.** The N-oxyl-4,4′-dimethyloxazolidine compounds were obtained from the corresponding keto acids by the method of Keana.[13] (Label I(5, 10) was first synthesized by Keith, *et al.*[14]) The keto acids were prepared according to Jones[15] (for the synthesis of the steroid labels, see ref 4).

**Preparation of the Esr Sample.** The spin labels were dissolved in ethanol and the solvent was evaporated in a small flask to give a thin film of spin label. The smectic phase was added and the sample stirred for about 5 min. The waxy material was then transferred into the esr cell by slightly applying suction. The inclusion of air bubbles could not be avoided. The final label concentration was about $10^{-4}$ mol label/1000 g of liquid crystalline phase, and all measurements were made at 20 ± 2°.

## IV. Experimental Results

Figure 1 shows two spectra which were obtained by doping the liquid crystalline phase with label I(13, 2) and orienting it by the procedure described above. There is a dramatic difference in the hyperfine splitting and the position of the spectrum, when the optical axis is parallel (Figure 1a) and perpendicular (Figure 1b) to the direction of the applied magnetic field. The comparison of the two spectra allows two qualitative conclusions. (1) The spin label undergoes a nanisotropic motion in the smectic phase. (2) The microcrystalline regions of phase D show a high degree of homogeneous orientation, though this ordering is not completely perfect (spectrum 1a still contains a very small contribution of spin labels which are oriented perpendicular to the bulk material). We attribute the inhomogeneities to edge effects in the sample cell and to the inclusion of air bubbles in the liquid crystalline phase.

The qualitative features of Figure 1 are equally valid for the rest of the spin labels of series I and II; however, there are remarkable quantitative differences in the observed hyperfine splittings and $g$ factors. Table I summarizes the quantitative evaluation of the different esr spectra. The meaning of the notation will become clear from Figure 1. (The last two columns in Table I refer to section VI.) The accuracy for $T_{||}$ and $T_{\perp}$ is about ±0.5 G and the relative accuracy of the $g$-factor measurements is ±0.0001. The orientation of the NO radical in the smectic phase—as described by the degree of order for the $x$, $y$, and $z$ axes—will be obtained by inserting the data of Table I into the appropriate equations of section II. (The approximate values for the $g$ factors are[12] $g_{xx} = 2.0089$, $g_{yy} = 2.0061$, $g_{zz} = 2.0027$.) The results of these calculations are represented in Table II. The relative errors amount to ±0.02 for $S_3$ and ±0.05 for $S_1$.

**Table I**

| Spin label | $T_{||}$ | $T_{\perp}$ | $a$ | $g_{||}$ | $g_{\perp}$ | $T_{max}$ Phase D | $T_{max}$ Phase Lipid |
|---|---|---|---|---|---|---|---|
| I(13, 2) | 26.1 | 9.5 | 15.0 | 2.0040 | 2.0068 | 26.2 | 26.6 |
| (12, 3) | 24.8 | 9.9 | 14.9 | 2.0042 | 2.0067 | 25.2 | 25.5 |
| (9, 6) | 20.1 | 11.9 | 14.6 | 2.0050 | 2.0065 | 21.0 | 24.9 |
| (5, 10) | 16.0 | 12.6 | 13.7 | 2.0056 | 2.0063 | | |
| (17, 3) | 24.7 | 10.4 | 15.0 | | | 25.1 | 25.5 |
| (0, 2) | 17.8 | 13.8 | 15.1 | | | | |
| IIa | 8.4 | 16.7 | 13.9 | 2.0062 | 2.0061 | | |
| IIb | 9.8 | 17.2 | 14.7 | | | | |

**Table II**

| Spin label | $T_{xx}$ | $T_{zz}$ | $S_3$ | $S_1$ | $S_2$ | $\bar{\theta}_3$, deg |
|---|---|---|---|---|---|---|
| I(13, 2) | 6.2 | 32.8 | 0.62 | −0.20 | −0.42 | 30.6 |
| (12, 3) | 6.1 | 32.4 | 0.56 | −0.17 | −0.39 | 32.5 |
| (9, 6) | 6.0 | 31.8 | 0.32 | −0.11 | −0.21 | 42.5 |
| (5, 10) | 5.6 | 29.9 | 0.14 | −0.06 | −0.08 | 49.5 |
| (17, 3) | 6.2 | 32.8 | 0.54 | | | |
| (0, 2) | 6.2 | 32.9 | 0.15 | | | |
| IIa | 5.7 | 30.4 | −0.34 | −0.30 | 0.64 | 70.7 |
| IIb | 6.1 | 32.1 | −0.28 | | | 67.7 |

**Table III**

| $\varphi$, deg | $T_{obsd}$ | $T_{theor}$ |
|---|---|---|
| 0 | 25.7 | 25.7 |
| 30 | 23.1 | 22.8 |
| 45 | 19.6 | 19.4 |
| 60 | 14.2 | 15.2 |
| 90 | 9.5 | 9.5 |

Table III compares experimental and theoretical results for the angular dependence of the hyperfine

(13) J. W. Keana, S. B. Keana, and D. Beetham, *J. Amer. Chem. Soc.*, 89, 3055 (1967).
(14) A. D. Keith, A. S. Waggoner, and O. H. Griffith, *Proc. Nat. Acad. Sci. U. S.*, 61, 819 (1968).
(15) R. G. Jones, *J. Amer. Chem. Soc.*, 69, 2350 (1947).

splitting of label I(13, 2) in phase D. In these measurements the magnetic field was rotated around the long axis of the sample cell, and $\varphi$ is the angle between the normal **n** on the cell face and the field direction. The theoretical values have been calculated with eq 7 under the assumption $T_{\varphi=0°} = T_{\parallel}$ and $T_{\varphi=90°} = T_{\perp}$. The agreement between experiment and theory supports the validity of this assumption and, consequently, the identity of **n** with the axis of motional averaging. The hyperfine splitting of the NO radical is rather sensitive to changes in solvent polarity. Table IV contains some

**Table IV**

| Solvent | $a$ |
|---|---|
| Water | 15.6 |
| Ethanol | 15.2 |
| Decanol | 14.2 |
| *n*-Decane | 13.9 |

typical values of the isotropic splitting constant $a$ for label I(9, 6) in different solvents. These numbers are only slightly different for the other labels of series I and II. Comparison of the various results obtained in phase D with the numbers in Table IV will help us to locate the position of the label with respect to the different regions of our model system.

## V. Discussion. The Anisotropic Motion of the Spin Labels and the Structure of the Model System

The experimental results presented in the foregoing section have made it clear that there is a homogeneous orientation of phase D in the sample cell and that the arrangement of the microcrystalline regions is of the type that has been anticipated from the optical polarization pattern (section I).

In the following discussion we therefore confine ourselves to the question of how the various labels are incorporated into the smectic phase and what information can be deduced about the molecular order of the bilayer. Let us begin with a discussion of the steroid labels II, where a straightforward and relatively simple explanation of the experimental data is possible. As has been mentioned above, the essential features of the steroid labels are their rigid structure and the unique way in which the NO group is attached to the steroid frame. The $y$ axis of the NO radical is extended along the long molecular axis so that $S_2$ not only refers to the NO group but at the same time describes the orientation of this molecular axis. If we now look at the actual numbers for label IIa (Table II), it follows from $S_2$ that the molecule is oriented almost parallel to the optical axis. The mean deviation from this axis amounts to only 20–25°. On the other hand, $S_1$ and $S_3$ are virtually equal within the limits of experimental accuracy, which proves an averaging of the $x$ and $z$ components of the **g** and **T** tensors. This averaging is due to a rapid rotation of the steroid label around its long axis. From the difference $(g_{xx} - g_{zz})$, which has to be averaged, one can estimate a lower limit of $10^8$ cps for the rotational frequency.

The isotropic splitting constant of label IIa in phase D corresponds to that in *n*-decane (Table IV). From this we conclude that the NO group is buried in the hydrophobic interior of the bilayer, while the OH group is anchored in the polar region.

The removal of the OH group, in label IIb, has only a minor influence on the high degree of order—as judged from $S_3$—but it switches the direction of the long molecular axis by 180°. Now the NO group is attached to the polar region which gives rise to a rather large isotropic splitting constant $a$.

From these experiments we can deduce a preliminary picture of our model system: the steroid labels must be embedded in parallel, rather extended hydrocarbon chains, which are in a state of rapid and highly anisotropic motion with a rotational frequency $>10^8$ cps.

We will now try to confirm and to refine this picture by examining the labels of series I. These labels behave very similarly to the amphiphilic materials of the bilayer phase in spite of the somewhat disturbing influence of the oxazolidine ring. Let us first turn our attention to the isotropic hyperfine splitting (Table I). As the position of the label group is moved toward the end of the hydrocarbon tail, a continuous decrease in the splitting constant $a$ can be observed. This gives some evidence that the orientation of the label molecule is the same as has been established for the unlabeled species, namely that the carboxyl group is in contact with the water phase while the hydrocarbon tail with the label group is tucked away into the hydrophobic region. Furthermore, the rather smooth decrease of the splitting constant indicates that the polar interface is not restricted to a planar surface but has a diffuse structure.

Additional details about the arrangement of the spin labels follow from an inspection of the $S$ values (Table II). The positive sign for $S_3$ shows that the nitrogen $2p\pi$ orbital must be oriented more or less parallel to the optical axis and, to a first approximation, this statement is equally valid for the orientation of the hydrocarbon chain. However, the interpretation of the $S$ values becomes more complicated because of the flexibility of the carbon skeleton. If the only configuration of the polymethylene chain were the planar *trans* form, then the nitrogen $2p\pi$ orbital should have the same degree of order at any point of the chain (we disregard label I(0, 2) for the moment). This is clearly not the case; instead we observe a decrease of order with increasing distance between the label group and the carboxyl end. But even with a spacing of ten carbon–carbon bonds between the two groups, we still detect a pronounced anisotropic motion of the label.

The molecular basis for the disordering is probably the rapid interconversion of the planar all-*trans* form with configurations which have substantial contributions from *gauche* conformations. Though an exact quantitative description of the flexibility should therefore be based on the rotational isomeric state model, preliminary insight can be gained by using the Porod–Kratky model,[16] which has the advantage of a simple mathematical formalism: we picture the polymethylene chain as a chain of freely jointed segments, which we numerate serially (Figure 2). The orientation of the first segment shall be fixed. To each subsequent segment we ascribe a Cartesian coordinate system such that the $z$ axis is extended along the direction of the

(16) O. Kratky and G. Porod, *Rec. Trav. Chim. Pays-Bas*, **68**, 1106 (1949).

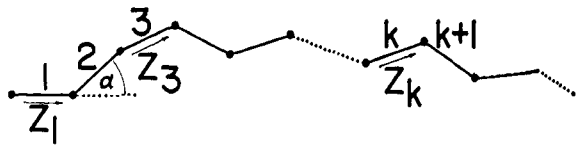


Figure 2.

segment. This axis is at the same time the direction of the $2p\pi$ orbital, if the NO group is attached to the respective segment. We make the assumption that each segment undergoes a symmetric rotation around the foregoing segment with a mean angular deviation $\alpha$. If this deviation has the same value for all the links, then the average position of any $z$ axis with respect to the foregoing can be given by the expression

$$S_\alpha = (1/2)(3\langle\cos^2\alpha\rangle - 1) \quad (17)$$

The degree of order $S_k$ of the $k$th segment with respect to the first coordinate system is obtained by the following procedure: we transform the $k$th coordinate system stepwise into the foregoing one and average during each step. This leads to the following result

$$S_k = (S_\alpha)^{k-1} \quad (18)$$

In our experimental situation, *i.e.*, in the case of an oriented spin label of type I, the first segment is not rigidly fixed, but shows some motion around the optical axis, described by the degree of order $S_0$. If we multiply eq 18 by $S_0$, we obtain a quantity which is experimentally accessible

$$S_k^* = S_0(S_\alpha)^{k-1} = S_3 \quad (19)$$

Equation 19 predicts that $S_3$ should depend exponentially on the number of carbon–carbon bonds between the label group and the carboxyl end. Figure 3 shows a plot of log $S_3$ against $k$. The diameter of the points corresponds to the accuracy of the measurement and the diagram shows a remarkable agreement with the prediction of our simple model. From the slope of the curve we calculate $S_\alpha = 0.82$ ($\alpha \approx 20°$). Label I(13, 2) deviates slightly from the predicted behavior in that the straight line in Figure 3 is bending off toward a smaller slope, indicating that the hydrocarbon chain becomes more rigid near the polar region.

According to eq 19, the length of the hydrocarbon tail following the label group should have no influence on $S_3$. This is in fact true for the labels I(17, 3) and I(12, 3) which show identical spectra, though the hydrocarbon tail of I(17, 3) is five segments longer than that of I(12, 3). But this statement is only of limited validity, because the length of the hydrocarbon end plays an important role in the solubility of the label in the hydrophobic region. Label I(0, 2), which has no hydrocarbon tail, is much less ordered by the liquid crystalline phase than the corresponding fatty acid label I(13, 2), thus giving a good illustration of this solubility effect.

The inspection of the $S_1$ and $S_2$ values (Table II) reveals another interesting feature. Since there is a remarkable difference between $S_1$ and $S_2$ for the labels I(13, 2) and I(12, 3), the $z$ axis of the NO group cannot coincide with the axis of rotational averaging. One possible model which is consistent with the experimental data is the following: the molecule is rotating around its long molecular axis, but the hydrocarbon chain shows a slight deformation thus giving rise to a

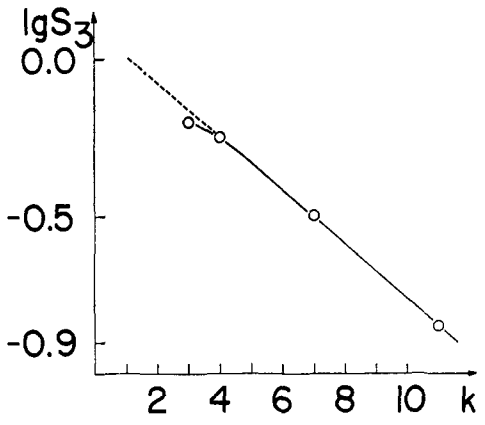


Figure 3. Dependence of the degree of order $S_3$ on the bond number $k$.

"pocket," which accommodates the bulky oxazolidine ring and by this minimizes the rotational resistance. This effect is concealed when the disorder of the chain increases [labels I(9, 6) and I(5, 10)].

To this point, we have concerned ourselves primarily with the flexibility of the polymethylene chain, giving perhaps the impression that this is somewhat contradictory to our previous model where the amphiphilic substances are in an extended state. But as can be seen from the following estimate, both interpretations are compatible: we assume a Porod–Kratky chain of $n$ segments, where all segments lie in one plane and deviate in the same direction. Then a lower limit of the end-to-end distance of the chain is given by

$$L = l(1 + \langle\cos\alpha\rangle + \langle\cos\alpha\rangle^2 + \ldots + \langle\cos\alpha\rangle^{n-1}) \quad (20)$$

where $l$ is the length of one segment. With $l = 1.27$ Å (the effective length of a carbon–carbon bond in a planar *trans* configuration) and with the approximation $\langle\cos\alpha\rangle \approx \langle\cos^2\alpha\rangle^{1/2}$ we obtain for a chain of nine segments (*e.g.*, *n*-decyl alcohol) $L \approx 9.0$–$10$ Å, which has to be compared with $L = 11.4$ Å for a completely rigid planar *trans* configuration. Thus, the intrinsic flexibility causes only a relatively small shortening of the chain. The slightly shorter chain seems to be more consistent with the measured bilayer thickness (22–24 Å) than the fully extended one, because the dimensions of the polar groups and the diffuse structure of the polar region yield additional increments to the bilayer dimensions. This would result in too large a spacing if an all-*trans* configuration of the carbon skeleton is assumed.

Finally, we want to point out that the end-to-end distance of liquid diiododecane has been determined by X-ray scattering to be 12.3 Å.[17] Substracting appropriate numbers for the iodine atoms yields a carbon–carbon end-to-end distance which is in good agreement with our estimate. We therefore conclude that though the hydrocarbon chains in our model system are in an almost extended configuration, it is justified to call this a "liquid" state.

(17) O. Kratky, G. Porod, and A. Sekora, *Monatsh. Chem.*, 78, 295 (1948).

## VI. A Comparison between Phospholipid Dispersions and Isotropic Distributions of Smectic Liquid Crystals

The investigation of the liquid crystalline model has resulted in a better quantitative understanding of the spin label behavior. We will now use this information to discuss some preliminary experiments with phospholipid dispersions. Such dispersions are similar to our model system in that the lipid molecules are packed into a bilayer arrangement, but they are at the same time different because of the special structure of the lipid molecules and because the bilayer is composed of a variety of different lipid species.

Since the phospholipid dispersions are not homogeneously oriented, a cylindrical sample cell was used for the liquid crystalline phase in order to obtain comparable spectra. This does not change the anisotropic rotation of the spin labels, but gives an isotropic distribution of the directions of the rotational axes. Figure 4a shows the resulting spectrum for label I(13, 2). Spectra of this type have been discussed quantitatively by McConnell.[3,5] According to this theory the splitting between the two outer peaks ($2T_{max}$ in Figure 4a) should correspond to $2T_{||}$ in an oriented sample—provided that the motion is highly anisotropic. The penultimate column in Table I contains the experimental $T_{max}$ values as determined from an isotropic distribution of the liquid crystalline phase. A comparison with the corresponding $T_{||}$ splittings reveals that the experimental results are consistent with the theoretical predictions.

We now turn to a short discussion of the behavior of our spin labels in phospholipid dispersions. The dispersions were prepared by ultrasonic irradiation of purified egg-yolk lecithin[18] in 0.1 *N* KCl/0.01 *M* Tris-HCl buffer at pH 8.5. We have used crude dispersions of multilamellar structure as well as vesicles consisting of one single bilayer.[19] The spin label results were exactly the same for both cases, which suggests that the bilayer structure is the only determining factor for the esr spectrum.

Figure 4b shows the spectrum of label I(13, 2) in such a lipid dispersion. It is almost identical with the spectrum of the model system. Since the line width is slightly broader in Figure 4b than in Figure 4a (causing the loss of resolution of the center peak), we conclude that the rotational frequency of the label is lower in the phospholipid dispersion than in our model system.

The very close similarity between the two systems is also true for the labels I(12, 3), I(5, 10), and I(17, 3) (*cf.* Table I; a quantitative evaluation in terms of $T_{max}$ is not possible for label I(5, 10), because the rotation is not sufficiently anisotropic). This suggests that these spin labels experience the same hydrocarbon environment in both situations; *i.e.*, they reflect the same organizational pattern for the lecithin dispersions and the model system, but they do not reveal any special lipid features.

(18) M. C. Pangborn, *J. Biol. Chem.*, 188, 471 (1951).
(19) C. Huang, *Biochemistry*, 8, 344 (1969).

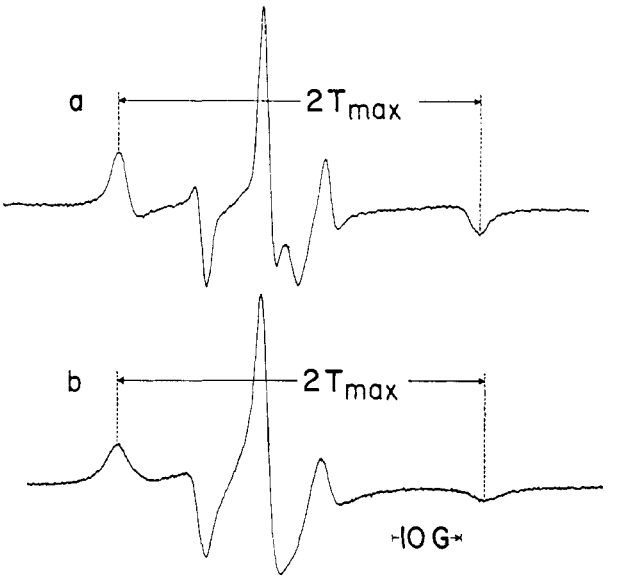


Figure 4. Spin label I(13, 2) in (a) isotropic distribution of smectic liquid crystals, and (b) dispersions of egg-yolk lecithin.

The only exception is label I(9, 6) which shows a larger anisotropy in the lipid system than in the liquid crystalline phase (Table I). Since the NO group is located, in this case, in a region of the phospholipid bilayer which is highly unsaturated, the higher rigidity is probably due to the influence of the double bonds, though the molecular mechanism of this effect is not yet clear.

This study has been conducted to obtain a better understanding of the potentialities and limits of spin-labeled molecules in bilayer systems. Some of the spin labels have already been incorporated in nerve membranes,[4,5] and the esr spectra indicate that the molecular order of at least parts of these biological membranes must have a close resemblance to that of the liquid crystalline model system. In concluding, we want to mention two other interesting aspects. (1) Our model system is a very suitable solvent system to determine the orientation of small molecules. (2) The spin labels of series I are a quite convenient means of studying the melting behavior of hydrocarbon chains. A detailed investigation of these subjects is in progress.

**Acknowledgment.** I am pleased to acknowledge my indebtedness to Professor H. M. McConnell for his introduction to the spin-labeling technique and many helpful discussions during the course of this work. I wish, also, to thank Dr. W. Hubbell for providing samples of the spin labels II and I(17, 3), and Dr. W. Balthasar for a sample of spin label I(0, 2).